

# Vesicle swelling regulates content expulsion during secretion

Marie L. Kelly<sup>1</sup>, Won Jin Cho<sup>1</sup>, Aleksandar Jeremic<sup>1</sup>,  
Rania Abu-Hamdah, Bhanu P. Jena\*

*Department of Physiology, Wayne State University School of Medicine, 5245 Scott Hall, 540 E. Canfield, Detroit, MI 48201, USA*

Received 10 July 2004; revised 11 July 2004; accepted 15 July 2004

## Abstract

The involvement of secretory vesicle swelling has been proposed in secretion; however, little is known about its role. Using both the pancreatic acinar cell and neuronal model, we show secretory vesicle swelling in live cells. Our study reveals that vesicle swelling potentiates its fusion at the cell plasma membrane, and is required for expulsion of intravesicular contents. Since the extent of swelling is directly proportional to the amount of vesicular contents expelled, this provides cells with the ability to regulate release of secretory products. These direct observations of the requirement of secretory vesicle swelling in secretion, provides an understanding of the appearance of partially empty vesicles following the process.

© 2004 International Federation for Cell Biology. Published by Elsevier Ltd. All rights reserved.

*Keywords:* Atomic force microscopy; Vesicle swelling; Secretion

## 1. Introduction

Resolving the molecular mechanism of cell secretion has been a challenge in biology. As part of the secretory process, little is known about the role of secretory vesicle swelling. Vesicle volume increase following stimulation of secretion is suggested from electrical measurements in mast cells (Fernandez et al., 1991; Curran and Brodwick, 1991; Monck et al., 1991; de Toledo et al., 1993), and recently demonstrated for digestive enzyme release from acinar cells of the exocrine pancreas (Cho et al., 2002a). Although electrophysiological measurements in mast cells suggest granule swelling to follow vesicle fusion at the plasma

membrane (Zimmerberg et al., 1987; Breckenridge and Almers, 1987), the potentiating effect of vesicle swelling on its fusion at the cell plasma membrane has also been recognized (Sattar et al., 2002; Finkelstein et al., 1986; Holz, 1986; Almers, 1990). It, however, remains unclear as to the primary role of secretory vesicle swelling in cell secretion. To address this issue, the pancreatic acinar cell and neurons were used in this study. Pancreatic acinar cells are polarized secretory cells, whose apical end possess specialized supramolecular structures called porosomes (Schneider et al., 1997; Cho et al., 2002b; Jena et al., 2003; Jeremic et al., 2003; Hörber and Miles, 2003) or fusion pores, where zymogen granules (ZGs), the membrane-bound secretory vesicles, dock and fuse to release their contents (Schneider et al., 1997; Cho et al., 2002b; Jena et al., 2003; Jeremic et al., 2003; Hörber and Miles, 2003). Our study reveals that vesicle swelling potentiates its fusion at the cell plasma membrane, and is required for expulsion of intravesicular contents.

\* Corresponding author. Tel.: +1 313 577 1532; fax: +1 313 993 4177.

E-mail address: [bjena@med.wayne.edu](mailto:bjena@med.wayne.edu) (B.P. Jena).

<sup>1</sup> Equal contribution.

## 2. Materials and methods

### 2.1. Isolation of pancreatic acinar cells

Isolation and preparation of acinar cells for atomic force microscopy (AFM) and electron microscopy (EM) were performed using minor modifications of a published procedure (Jena et al., 1991). For each experiment, a male Sprague–Dawley rat weighing 80–100 g was euthanized by carbon dioxide inhalation. The pancreas was excised and chopped into 0.5-mm<sup>3</sup> pieces, which were mildly agitated for 10 min at 37 °C in a siliconized glass tube with 5 ml of oxygenated buffer A (98 mM NaCl, 4.8 mM KCl, 2 mM CaCl<sub>2</sub>, 1.2 mM MgCl<sub>2</sub>, 0.1% bovine serum albumin, 0.01% soybean trypsin inhibitor, 25 mM Hepes, pH 7.4) containing 1000 units of collagenase. The suspension of acini was filtered through a 224 µm Spectra-Mesh (Spectrum Laboratory Products, Saint Paul, MN, U.S.A.) polyethylene filter to remove large clumps of acini and undissociated tissue. The acini were washed six times, 50 ml per wash, with ice-cold buffer A. Isolated rat pancreatic acini and acinar cells were plated on Cell-Tak-coated (Collaborative Biomedical Products, Bedford, MA, U.S.A.) glass coverslips or mica. After plating (2–3 h), cells were imaged by the AFM before and during stimulation of secretion. Isolated acinar cells and small acinar preparations were used in the study because fusions of regulated secretory vesicles at the cell plasma membrane in pancreatic acini were confined to the apical region and are impossible to image by the AFM in whole tissue or large acinar preparations.

### 2.2. Preparation of zymogen granules

Zymogen granules were isolated according to a published procedure with minor modification (Jena et al., 1997). The pancreas from male Sprague–Dawley rats was dissected and diced into 0.5-mm<sup>3</sup> pieces before being suspended into 15% (wt/vol) ice-cold homogenization buffer (0.3 M sucrose, 25 mM Hepes, pH 6.5, 1 mM benzamidine, 0.01% soybean trypsin inhibitor) and homogenized using three strokes of a Teflon-glass homogenizer. The homogenate was centrifuged for 5 min at 300 × g at 4 °C. The supernatant fraction was mixed with two volumes of a Percoll–Sucrose–Hepes buffer (0.3 M sucrose, 25 mM Hepes, pH 6.5, 86% Percoll, 0.01% soybean trypsin inhibitor) and centrifuged for 30 min at 16,400 × g at 4 °C. Pure ZGs were obtained as a loose white pellet at the bottom of the centrifuge tube, and used in the study.

### 2.3. Immunoisolation of the porosome complex

Fusion pores were immunoisolated from pancreatic plasma membrane preparations using our published procedure (Jena et al., 2003; Jeremic et al., 2003).

### 2.4. Preparation of porosome-reconstituted bilayer

Planar lipid bilayers with a capacitance between 100 and 270 pF were formed by brushing 7:3 by weight phosphatidylcholine:phosphatidylserine from brain (Avanti Polar Lipids, Alabaster, AL) which had been dried and resuspended in decane (20 mg lipid/ml decane) onto the *cis* side of the hole of a bilayer cup inserted into a bilayer chamber (Warner Instruments). Bath solution was symmetric 150 mM KCl, 20 mM 2-*N* morpholinoethanesulfonic acid (MES), 1 mM CaCl<sub>2</sub>, pH 6.5. Capacitance, membrane conductance and bilayer current were recorded for 3–5 min using an EPC9 patch clamp setup and pulse software (HEKA) and ascertained for stability before incorporating porosome into the bilayer membrane using the brush technique (Jeremic et al., 2003).

### 2.5. Bilayer fusion assay

Zymogen granules were added to the *cis* side of the bilayer chamber. GTP was added before removal of either the 15 min ( $n = 5$ ) or 30 min ( $n = 5$ ) time points. For each experiment, 75 µl samples were removed from the *trans* side of the bilayer chamber for  $\alpha$ -amylase immunoblot analysis. Following GTP addition, samples were removed at ~0, 5, 10, 15, 30 and 35 min. Capacitance, membrane conductance and bilayer current were continually monitored and recorded during the experiment using an EPC9 patch clamp system in conjunction with the bilayer setup and pulse software (HEKA).

### 2.6. Transmission electron microscopy

Isolated rat pancreatic acini, ZGs, and brain tissue fractions were fixed in 2.5% buffered paraformaldehyde (PFA) for 30 min, and the pellets were embedded in Unicryl resin and were sectioned at 40–70 nm. Thin sections were transferred to coated specimen transmission electron microscopy (TEM) grids, dried in the presence of uranyl acetate and methyl cellulose, and examined in a transmission electron microscope.

### 2.7. AFM volume measurements of ZGs

Isolated ZGs in 125 mM KCl–MES buffer (25 mM KCl, 100 mM 2-*N* morpholinoethanesulfonic acid), pH 6.5 were plated on Cell-Tak-coated glass coverslips or mica. After plating (10 min), the coverslips were placed in a fluid chamber and washed with the KCl–MES buffer to remove unattached vesicles, prior to imaging the attached ZGs in KCl–MES buffer, in the presence or absence of 1 µM, 5 µM, 10 µM and, 20 µM GTP. ZG imaging and dynamics were performed using the Nanoscope IIIa, an atomic force microscope from Digital Instruments (Santa Barbara, CA). ZGs were imaged both in the “contact” and “tapping” mode in fluid (Jena et al.,

1997, 2003). However, all images presented in this report were obtained in the “tapping” mode in fluid, using silicon nitride tips with a spring constant of  $0.06 \text{ Nm}^{-1}$  and an imaging force of less than  $200 \text{ pN}$ . Images were obtained at line frequencies of  $2.523 \text{ Hz}$ , with 512 lines per image and constant image gains. GTP dose-dependent, morphological changes in ZGs were obtained by using section analysis. Topographical dimensions of ZGs were analyzed with the software NANOSCOPE (R) IIIA 4.43r8 supplied by Digital Instruments.

### 2.8. Isolation of synaptosomes, synaptosomal membrane and synaptic vesicles

Synaptosomes, synaptosomal membrane and synaptic vesicles were prepared from rat brains (Jeong et al., 1998; Thoidis et al., 1998). Whole rat brain from Sprague–Dawley rats (100–150 g) were isolated and placed in ice-cold buffered sucrose solution (5 mM Hepes pH 7.4, 0.32 M sucrose) supplemented with protease inhibitor cocktail (Sigma, St. Louis, MO) and homogenized using Teflon-glass homogenizer (8–10 strokes). The total homogenate was centrifuged for 3 min at  $2500 \times g$ . The supernatant fraction was further centrifuged for 15 min at  $14,500 \times g$ , and the resultant pellet was resuspended in buffered sucrose solution, which was loaded onto 3–10–23% Percoll gradients. After centrifugation at  $28,000 \times g$  for 6 min, the enriched synaptosomal fraction was collected at the

10–23% Percoll gradient interface. To isolate synaptic vesicles and synaptosomal membrane (Thoidis et al., 1998), isolated synaptosomes were diluted with nine volumes of ice-cold  $\text{H}_2\text{O}$  (hypotonic lysis of synaptosomes to release synaptic vesicles) and immediately homogenized with three strokes in a Dounce homogenizer, followed by a 30 min incubation on ice. The homogenate was centrifuged for 20 min at  $25,500 \times g$ , and the resultant pellet (enriched synaptosomal membrane preparation) and supernatant (enriched synaptic vesicles preparation) were used in our studies.

### 2.9. Light scattering measurements of changes in synaptic vesicle size

Kinetics of rat synaptic vesicle volume changes were monitored by  $90^\circ$  light scattering with excitation and emission wavelength set at  $400 \text{ nm}$  in a Hitachi F-2000 spectrophotometer. Synaptic vesicle suspension was injected into the thermo-regulated cuvette containing  $700 \mu\text{l}$  of a buffer solution (NaCl 140 mM; KCl 2.5 mM;  $\text{NaH}_2\text{PO}_4$  0.25 mM;  $\text{KH}_2\text{PO}_4$  0.25 mM; pH 7.4) at  $37^\circ\text{C}$ . Light scattering was monitored for 1 min following addition of synaptic vesicles to either buffer alone (control) or buffer containing the heterotrimeric Gi-protein agonist, mastoparan (experimental) or its non-agonistic control peptide, Mast-17 (control). Values are expressed as percent increase in light scattered over control values.

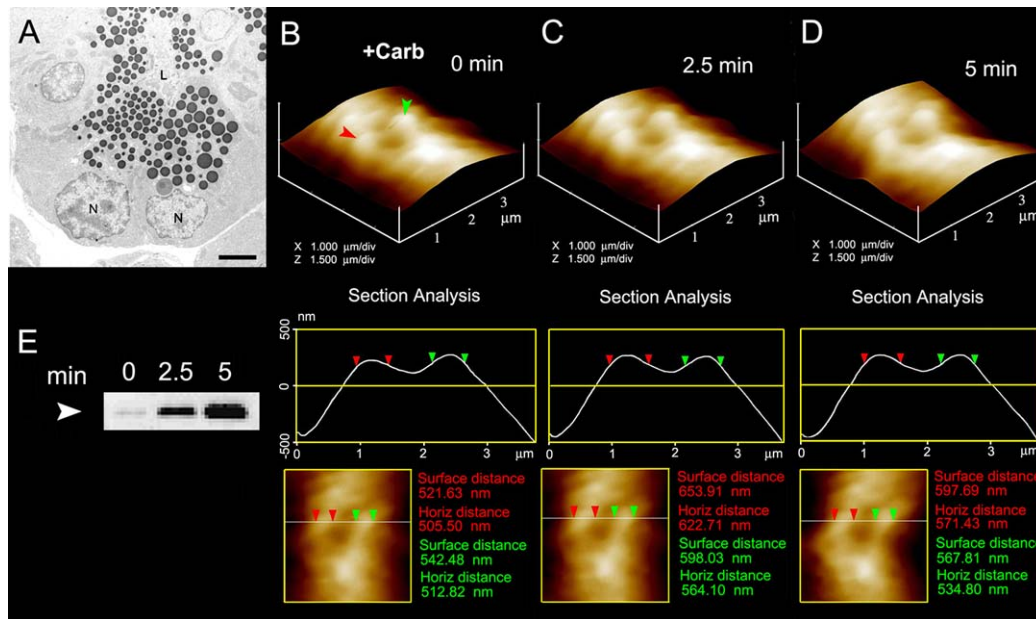


Fig. 1. The swelling dynamics of ZGs in live pancreatic acinar cells. (A) Electron micrograph of pancreatic acinar cells showing the basolaterally located nucleus (N) and the apically located ZGs. The apical end of the cell faces the acinar lumen (L). Bar =  $2.5 \mu\text{m}$ . (B–D) The apical ends of live pancreatic acinar cells were imaged by AFM, showing ZGs (red and green arrowheads) lying just below the apical plasma membrane. Exposure of the cell to a secretory stimulus using  $1 \mu\text{M}$  carbamylcholine, resulted in ZG swelling within 2.5 min, followed by a decrease in ZG size after 5 min ( $n = 8$ ). The decrease in size of ZGs after 5 min is due to the release of secretory products such as  $\alpha$ -amylase, as demonstrated by the immunoblot assay (E).

### 3. Results and discussion

Pancreatic acinar cells (Fig. 1A) were used in this study. Isolated live pancreatic acinar cells in near physiological buffer were imaged using the atomic force microscope (AFM) at high force (200–300 pN), to image ZGs lying immediately below the apical plasma membrane of the cell (Fig. 1B). Within 2.5 min of exposure to a physiological secretory stimulus (1  $\mu$ M carbamylcholine), the majority of ZGs within cells swell (Fig. 1C), followed by a decrease in ZG size (Fig. 1D) by which time most of the release of secretory products from within ZGs had occurred (Fig. 1E). These studies reveal for the first time in live cells, intracellular swelling of secretory vesicles following stimulation of secretion and their deflation following partial discharge of vesicular contents. Measurements of intracellular ZG size further reveal that different vesicles swell differently, following a secretory stimulus. For example, the ZG marked by the red arrowhead swelled to show a 23–25% increase in diameter, in contrast to the green arrowhead-marked ZG which increased by only 10–11% (Fig. 1B, C). This differential swelling among ZGs within the same cell, may explain why following stimulation of secretion, some intracellular ZGs demonstrate the presence of less vesicular content than others, and hence have discharged more of their contents (Cho et al., 2002a).

To determine precisely the role of swelling in vesicle–plasma membrane fusion and in the expulsion of intravesicular contents, an electrophysiological ZG-reconstituted lipid bilayer fusion assay (Jeremic et al., 2003) was employed. The ZGs used in the bilayer fusion

assays were characterized for their purity and their ability to respond to a swelling stimulus. ZGs were isolated (Jena et al., 1997) and their purity assessed using electron microscopy (Fig. 2A). As previously reported (Jena et al., 1997; Cho et al., 2002c; Abu-Hamdah et al., 2004), exposure of isolated ZGs (Fig. 2B) to GTP resulted in ZG swelling (Fig. 2C). Once again, similar to what is observed in live acinar cells (Fig. 1), each isolated ZG responded differently to the same swelling stimulus. For example, the red arrowhead points to a ZG whose diameter increased by 29% as opposed to the green arrowhead pointing ZG that increased only by a modest 8%. The differential response of isolated ZGs to GTP was further assessed by measuring the changes in the volume of isolated ZGs of different size (Fig. 2D). ZGs in the exocrine pancreas range in size from 0.2 to 1.3  $\mu$ m in diameter (Jena et al., 1997). Not all ZGs were found to swell following a GTP challenge. Most ZGs volume increases were between 5 and 20%. However, larger increases (up to 45%) were observed only in vesicles ranging from 250 to 750 nm in diameter (Fig. 2D). These studies demonstrate that following stimulation of secretion, ZGs within pancreatic acinar cells swell, followed by a release of intravesicular contents through porosomes (Jeremic et al., 2003) at the cell plasma membrane, and a return to resting size on completion of secretion. On the contrary, isolated ZGs stay swollen following exposure to GTP, since there is no release of the intravesicular contents. In acinar cells, little or no secretion was detected 2.5 min following stimulation of secretion, although the ZGs within them were completely swollen (Fig. 1C). However, at 5 min following stimulation, ZGs deflated and the intravesicular  $\alpha$ -amylase

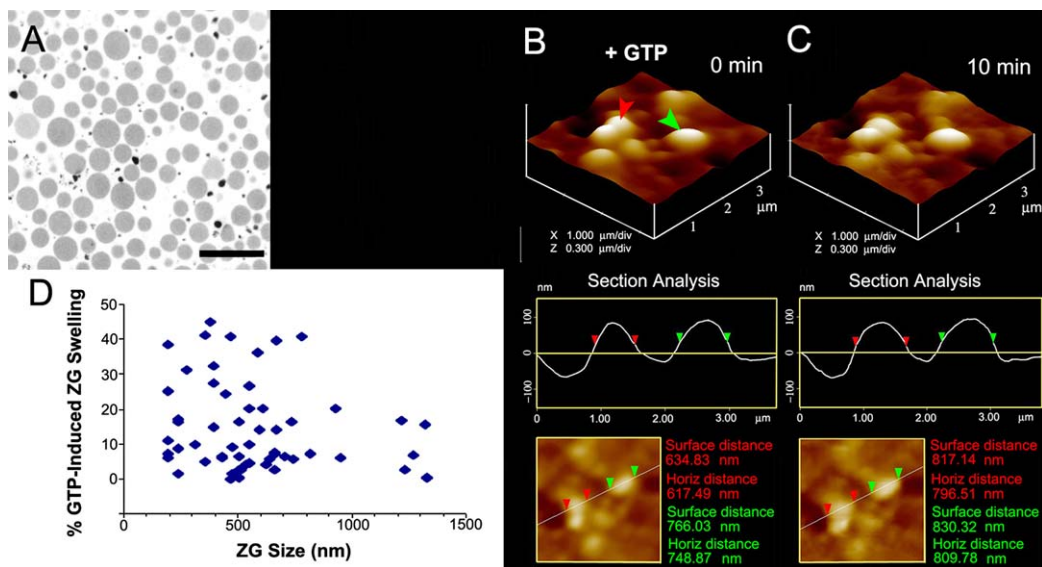


Fig. 2. Swelling of isolated ZGs. (A) Electron micrograph of isolated ZGs demonstrating a homogeneous preparation. Bar = 2.5  $\mu$ m. (B, C) Isolated ZGs, on exposure to 20  $\mu$ M GTP, swell rapidly. Note the enlargement of ZGs as determined by AFM section analysis of two vesicles (red and green arrowheads). (D) Percent ZG volume increase in response to 20  $\mu$ M GTP. Note how different ZGs respond to the GTP-induced swelling differently.

released from the acinar cell was detected, suggesting the involvement of ZG swelling in secretion.

In the electrophysiological bilayer fusion assay, immunisolated fusion pores or porosomes from the exocrine pancreas were isolated and functionally reconstituted (Jeremic et al., 2003) into the lipid membrane of the bilayer apparatus, where membrane conductance and capacitance were continually monitored (Fig. 3A). Reconstitution of the porosome into the lipid membrane resulted in a small increase in capacitance (Fig. 3B), possibly due to the increase in membrane surface area contributed by incorporation of porosomes, ranging in size from 100 to 150 nm in diameter (Jeremic et al., 2003). Isolated ZGs when added to the *cis* compartment of the bilayer chamber, fuse at the porosome-reconstituted lipid membrane (Fig. 3A) and was detected as a step increase in membrane capacitance (Fig. 3B). However, even after 15 min of ZG addition to the *cis* compartment of the bilayer chamber, little or no release of the intravesicular enzyme  $\alpha$ -amylase was detected in the *trans* compartment of the chamber (Fig. 3C, D). On the contrary, exposure of ZGs to 20  $\mu$ M GTP, induced swelling (Jena et al., 1997; Cho et al., 2002c; Abu-Hamdah et al., 2004) and resulted in both the potentiation of fusion and a robust expulsion of  $\alpha$ -amylase into the *trans* compartment of the bilayer chamber (Fig. 3C, D). These studies demonstrated that during secretion, secretory vesicle swelling is required for the efficient expulsion of intravesicular contents.

Within minutes or even seconds following stimulation of secretion, empty and partially empty secretory vesicles accumulate within cells (Cho et al., 2002a; Lawson et al., 1975; Plattner et al., 1997). There may be two possible explanations for such accumulation of partially empty vesicles. Following fusion at the porosome, secretory vesicles may either remain fused for a brief period and therefore time would be the limiting factor for partial expulsion, or inadequately swell and therefore unable to generate the required intravesicular pressure for complete discharge. Our results in Fig. 3 suggest that it would be highly unlikely that generation of partially empty vesicles result from brief periods of vesicle fusion at porosomes. After addition of ZGs to the *cis* chamber of the bilayer apparatus, membrane capacitance continued to increase, however, little or no detectable secretion occurred even after 15 min (Fig. 3), suggesting that either variable degrees of vesicle swelling or repetitive cycles of fusion and swelling of the same vesicle or both, may operate during secretion. Under these circumstances, empty and partially empty vesicles could be generated within cells following secretion. To test this hypothesis, we examined two key parameters. One, whether the extent of swelling is the same for all ZGs exposed to a certain concentration of GTP. Two, whether ZGs are capable of swelling to different degrees.

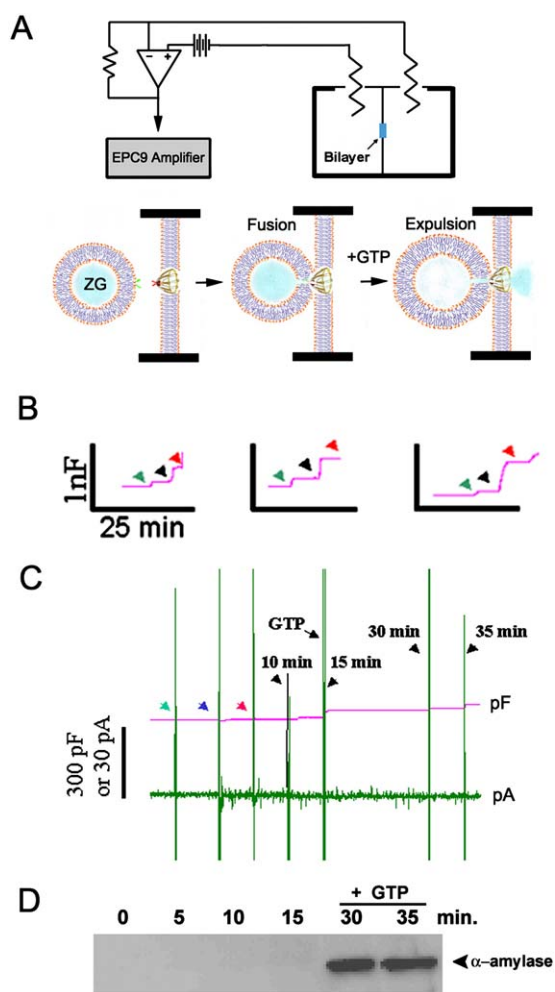


Fig. 3. Fusion of isolated ZGs at porosome-reconstituted bilayer and GTP-induced expulsion of  $\alpha$ -amylase. (A) Schematic diagram of the EPC9 bilayer apparatus showing the *cis* and *trans* chambers. Isolated ZGs when added to the *cis* chamber, fuse at the bilayers-reconstituted porosome. Addition of GTP to the *cis* chamber induces ZG swelling and expulsion of its contents such as  $\alpha$ -amylase to the *trans* bilayers chamber (B) Capacitance traces of the lipid bilayer from three separate experiments following reconstitution of porosomes (green arrowhead), addition of ZGs to the *cis* chamber (blue arrowhead), and the red arrowhead represents the 5 min time point after ZG addition. Note the small increase in membrane capacitance following porosome reconstitution, and a greater increase when ZGs fuse at the bilayers. (C) In a separate experiment, 15 min after addition of ZGs to the *cis* chamber, 20  $\mu$ M GTP was introduced. Note the increase in capacitance, demonstrating potentiation of ZG fusion. Flickers in current trace represent current activity. (D) Immunoblot analysis of  $\alpha$ -amylase in the *trans* chamber fluid at different times following exposure to ZGs and GTP. Note the undetectable levels of  $\alpha$ -amylase even up to 15 min following ZG fusion at the bilayer. However, following exposure to GTP, significant amounts of  $\alpha$ -amylase from within ZGs were expelled into the *trans* bilayers chamber. ( $n = 6$ ).

And if so, whether there is a correlation between extent of swelling and the quantity of intravesicular contents expelled. The answer to the first question is clear, that different ZGs respond to the same stimulus differently (Fig. 1). Our study revealed that different ZGs within

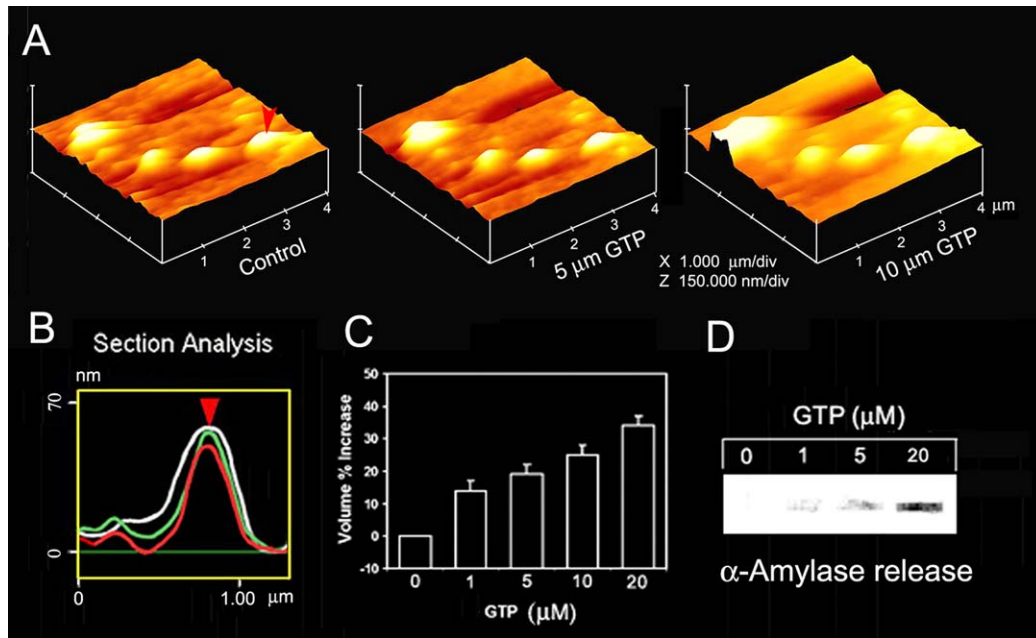


Fig. 4. The extent of ZG swelling is directly proportional to the amount of intravesicular contents released. (A) AFM micrographs showing the GTP dose-dependent increase in swelling of isolated ZGs. (B) Note the AFM section analysis of a single ZG (red arrowhead), showing the height and relative width at resting (control, red outline), following exposure to 5 μM GTP (green outline) and 10 μM GTP (white outline). (C) Graph demonstrating the GTP dose-dependent percent increase in ZG volume ( $n = 16$ ). Data are expressed as mean  $\pm$  SEM. (D) Immunoblot analysis of  $\alpha$ -amylase in the *trans* chamber fluid of the bilayers chamber following exposure to different doses of GTP. Note the GTP dose-dependent increase in  $\alpha$ -amylase release from within ZGs fused at the *cis* side of the reconstituted bilayer.

cells or in isolation undergo different degrees of swelling, even though they are exposed to the same stimuli (carbamylcholine for live pancreatic acinar cells) or GTP for isolated ZGs (Figs. 1B–D, 2B–D). The

requirement of ZG swelling for expulsion of vesicular contents was further confirmed, when the GTP dose-dependently increased ZG swelling (Fig. 4A–C) translated into increased secretion of  $\alpha$ -amylase

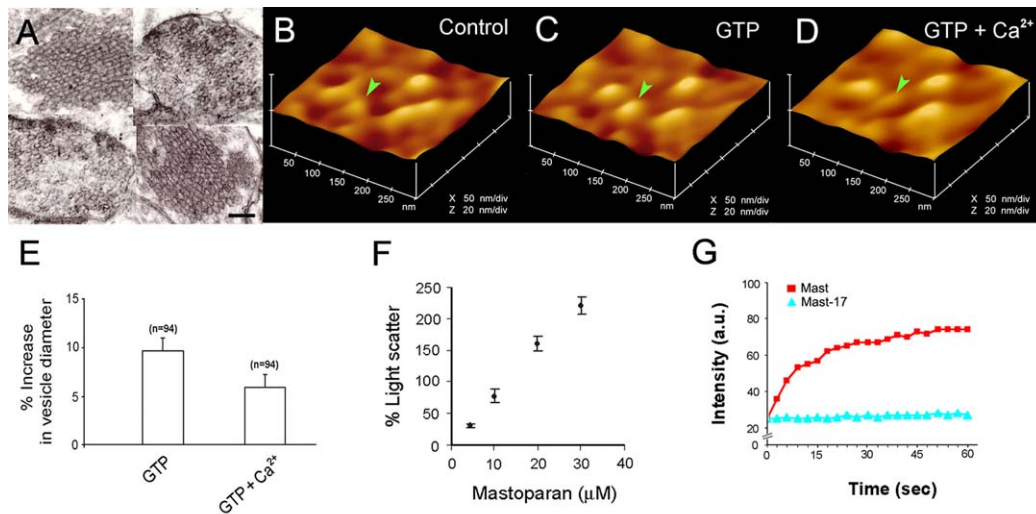


Fig. 5. Synaptic vesicles swell in response to GTP and mastoparan, and vesicle swelling is required for neurotransmitter release. (A) Electron micrographs of brain synaptosomes, demonstrating the presence of 40–50 nm synaptic vesicles within. Bar = 200 nm. (B) AFM micrographs of synaptosomal membrane, demonstrating the presence of 40–50 nm synaptic vesicles docked to the cytosolic face of the presynaptic membrane. (C) Exposure of the synaptic vesicles to 20 μM GTP results in vesicle swelling (blue arrowhead). (D, E) Further addition of calcium results in the transient fusion of the synaptic vesicles at porosomes in the presynaptic membrane of the nerve terminal, and expulsion of intravesicular contents. Note the decrease in size of the synaptic vesicle following content expulsion ( $n = 94$ ). Data are expressed as mean  $\pm$  SEM.  $P < 0.01$ . (F) Light scattering assays on isolated synaptic vesicles demonstrate the mastoparan dose-dependent increase in vesicle swelling ( $n = 5$ ), and further confirm the AFM results. (G) Exposure of isolated synaptic vesicles to 20 μM mastoparan demonstrates a time-dependent (in seconds) increase in their swelling. Note the control peptide mast-17 has little or no effect on synaptic vesicle swelling.

(Fig. 4D). Although higher GTP concentrations elicited an increased ZG swelling, the extent of swelling between ZGs once again varied.

To determine if a similar or an alternate mechanism is responsible for the release of secretory products in a fast secretory cell, synaptosomes and synaptic vesicles from rat brain were used in the study. Since synaptic vesicle membrane is known to possess both Gi and Go proteins, we hypothesized GTP and Gi-agonist (mastoparan) mediated vesicle swelling. To test this hypothesis, isolated synaptosomes (Fig. 5A) were lysed to obtain synaptic vesicles and synaptosomal membrane. Isolated synaptosomal membrane when placed on mica and imaged by the AFM in near physiological buffer, reveals on the cytosolic side the presence of 40–50 nm in diameter synaptic vesicles still docked to the presynaptic membrane. Similar to the ZGs, exposure of synaptic vesicles (Fig. 5B) to 20  $\mu$ M GTP (Fig. 5C), resulted in an increase in synaptic vesicle swelling. However, exposure to  $Ca^{2+}$  results in the transient fusion of synaptic vesicles at the presynaptic membrane, expulsion of intravesicular contents, and the consequent decrease in size of the synaptic vesicle (Fig. 5D, E). In Fig. 5B–D, the blue arrowhead points to a synaptic vesicle undergoing this process. Additionally, as observed in ZGs of the exocrine pancreas, not all synaptic vesicles swell, and if they do, they swell to different extents even though they had been exposed to the same stimuli. This differential response of synaptic vesicles within the same nerve ending may dictate and regulate the potency and efficacy of neurotransmitter release at the nerve terminal. To further confirm synaptic vesicle swelling and determine the swelling rate, light scattering experiments were performed. Light scattering studies demonstrate a mastoparan dose-dependent increase in synaptic vesicle swelling (Fig. 5F). Mastoparan (20 mM) induces a time-dependent (in seconds) increase in synaptic vesicle swelling (Fig. 5G), as opposed to the control peptide (Mast-17).

In this report we show that following stimulation of secretion, ZGs, the membrane-bound secretory vesicles in exocrine pancreas swell. Different ZGs swell differently, and the extent of their swelling dictates the amount of intravesicular contents to be expelled. ZG swelling is therefore a requirement for the expulsion of vesicular contents in the exocrine pancreas. Similar to ZGs, swelling of synaptic vesicles enable the expulsion of neurotransmitters at the nerve terminal. This mechanism of vesicular expulsion during cell secretion may explain why partially empty vesicles are observed in secretory cells (Cho et al., 2002a; Lawson et al., 1975; Plattner et al., 1997) following secretion. The presence of empty secretory vesicles could result from multiple rounds of fusion–swelling–expulsion, a vesicle may undergo during the secretory process. These results reflect the precise and regulated nature of cell secretion, from the exocrine pancreas to neurons.

## Acknowledgments

This work was supported by NIH grants DK56212 and NS39918 (B.P.J.).

## References

- Abu-Hamdah R, Cho WJ, Cho SJ, Jeremic A, Kelly M, Ilie AE, et al. Regulation of the water channel aquaporin-1: isolation and reconstitution of the regulatory complex. *Cell Biol Int* 2004;28:7–17.
- Almers W. Exocytosis. *Annu Rev Physiol* 1990;52:607–24.
- Breckenridge LJ, Almers W. Final steps in exocytosis observed in a cell with giant secretory granules. *Proc Natl Acad Sci U S A* 1987;84:1945–9.
- Cho S-J, Cho J, Jena BP. The number of secretory vesicles remains unchanged following exocytosis. *Cell Biol Int* 2002a;26:29–33.
- Cho SJ, Quinn AS, Stromer MH, Dash S, Cho J, Taatjes DJ, et al. Structure and dynamics of the fusion pore in live cells. *Cell Biol Int* 2002b;26:35–42.
- Cho SJ, Sattar AK, Jeong EH, Satchi M, Cho JA, Dash S, et al. Aquaporin 1 regulates GTP-induced rapid gating of water in secretory vesicles. *Proc Natl Acad Sci U S A* 2002c;99:4720–4.
- Curran MJ, Brodwick MS. Ionic control of the size of the vesicle matrix of beige mouse mast cells. *J Gen Physiol* 1991;98:771–90.
- Fernandez JM, Villalon M, Verdugo P. Reversible condensation of mast cell secretory products in vitro. *Biophys J* 1991;59:1022–7.
- Finkelstein A, Zimmerberg J, Cohen FS. Osmotic swelling of vesicles: its role in the fusion of vesicles with planar phospholipid bilayer membranes and its possible role in exocytosis. *Annu Rev Physiol* 1986;48:163–74.
- Holz RW. The role of osmotic forces in exocytosis from adrenal chromaffin cells. *Annu Rev Physiol* 1986;48:175–89.
- Hörber JKH, Miles MJ. Scanning probe evolution in biology. *Science* 2003;302:1002–5.
- Jena BP, Cho SJ, Jeremic A, Stromer MH, Abu-Hamdah R. Structure and composition of the fusion pore. *Biophys J* 2003;84:1337–43.
- Jena BP, Padfield PJ, Ingebritsen TS, Jamieson JD. Protein tyrosine phosphatase stimulates  $Ca^{2+}$ -dependent amylase secretion from pancreatic acini. *J Biol Chem* 1991;266:17744–6.
- Jena BP, Schneider SW, Geibel JP, Webster P, Oberleithner H, Sritharan KC. Gi regulation of secretory vesicle swelling examined by atomic force microscopy. *Proc Natl Acad Sci U S A* 1997;94:13317–22.
- Jeong E-H, Webster P, Khuong CQ, Sattar AKMA, Satchi M, Jena BP. The native membrane fusion machinery in cells. *Cell Biol Int* 1998;22:657–70.
- Jeremic A, Kelly M, Cho SJ, Stromer MH, Jena BP. Reconstituted fusion pore. *Biophys J* 2003;85:2035–43.
- Lawson D, Fewtrell C, Gomperts B, Raff MC. Anti-immunoglobulin-induced histamine secretion by rat peritoneal mast cells studied by immunoferritin electron microscopy. *J Exp Med* 1975;142:391–401.
- Monck JR, Oberhauser AF, Alvarez de Toledo G, Fernandez JM. Is swelling of the secretory granule matrix the force that dilates the exocytotic fusion pore? *Biophys J* 1991;59:39–47.
- Plattner H, Artalejo AR, Neher E. Ultrastructural organization of bovine chromaffin cell cortex—analysis by cryofixation and morphometry of aspects pertinent to exocytosis. *J Cell Biol* 1997;139:1709–17.
- Sattar AK, Boinpally R, Stromer MH, Jena BP. Galpha(i3) in pancreatic zymogen granules participates in vesicular fusion. *J Biochem* 2002;131:815–20.

- Schneider SW, Sritharan KC, Geibel JP, Oberleithner H, Jena BP. Surface dynamics in living acinar cells imaged by atomic force microscopy: identification of plasma membrane structures involved in exocytosis. *Proc Natl Acad Sci U S A* 1997;94:316–21.
- Thoidis G, Chen P, Pushkin AV, Vallega G, Leeman SE, Fine RE, et al. Two distinct populations of synaptic-like vesicles from rat brain. *Proc Natl Acad Sci U S A* 1998;95:183–8.
- de Toledo G Alvarez, Fernandez-Chacon R, Fernandez JM. Release of secretory products during transient vesicle fusion. *Nature* 1993; 363:554–8.
- Zimmerberg J, Curran M, Cohen FS, Brodwick M. Simultaneous electrical and optical measurements show that membrane fusion precedes secretory granule swelling during exocytosis of beige mouse mast cells. *Proc Natl Acad Sci U S A* 1987;84:1585–9.